Available online at www.sciencedirect.com
ScienceDirect
Journal of the European Ceramic Society 27 (2007) 319–326
www.elsevier.com/locate/jeurceramsoc

Mechanical properties and microstructures of hot-pressed MgAlON–BN composites

Zuotai Zhang [a], Lidong Teng [a,*], Wenchao Li [b]

[a] *Department of Materials Science and Engineering, Royal Institute of Technology, Brinellvägen 23, 100 44, SE-10044 Stockholm, Sweden*
[b] *Department of Physical Chemistry, University of Science and Technology, Beijing 100083, People's Republic of China*

Received 23 November 2005; received in revised form 10 April 2006; accepted 29 April 2006
Available online 13 July 2006

Abstract

The relationship between the mechanical properties and microstructure of hot-pressed MgAlON–BN composite materials was investigated by scanning electron microscopy (SEM), transmission electron microscopy (TEM), high resolution electron microscopy (HREM) and X-ray diffraction (XRD) techniques. The phase compositions of hot-pressed samples prepared from starting mixtures of Al_2O_3, AlN, MgO and h–BN consisted of MgAlON phases as a matrix and BN phases as the second phase. The density, bending strength at room temperature, fracture toughness and Vickers hardness were measured. The results indicated that the density, strength and Vickers hardness decrease with increasing h–BN content due to the non-reactive nature and layered structure of h–BN. The fracture toughness, however increased with increasing h–BN addition, reaching a maximum of 3.64 MPa $m^{0.5}$; it decreased with further increase of BN content. The increase of fracture toughness was attributed to the presence of microcracks and the decrease was considered to be the discontinuous microstructure of the MgAlON phases. Temperature dependence of bending strength remained constant at low temperature, followed by an increase at 800 °C and then, dropped quickly. The increase in the bending strength of the composite was attributed to the decrease of residual stress and to the interwoven microstructure of the composites which prevented grain boundary slip and reduced the attenuation rate of high temperature strength. The machinability of the composites was examined. The results indicate that the composite materials with BN content more than 15 vol.% exhibit excellent machinability and could be drilled using conventional hard metal alloy drills.

Keywords: Mechanical properties; Microstructure; Hot pressing; Composites; Refractories; BN; MgAlON

1. Introduction

Mechanical properties including the ability to support loads and compressive stress are important properties for high performance structural composite ceramics and advanced refractories. The mechanical properties are mainly determined by the microstructure in composite ceramics—the phase components and the composition of grain boundary phases as well as residual stress and microcracks.[1,2] Crystallization and vitrification effects, however, have pronounced effect on three point bending strength.[3,4] Machining is emerging as an important requirement for the flexible use of high performance refractories. In order to improve the machinability of composite ceramics, one of the methods is to introduce a weak interface phase or layered structure into the matrix to facilitate crack deflection and propagation during machining.[5,6]

Hexagonal graphitic boron nitride (h–BN) composites show excellent corrosion and thermal shock resistance, good mechanical tolerance and machinability.[6] Si_3N_4–BN[7–9] and Sialon–BN[10] composites have already been used as special refractory nozzles, tubes and break rings for the continuous casting of steel. However, the decomposition of Si_3N_4 and Sialon by dissolution of silicon into molten steel restricted their wide application.[11] In order to get rid of these shortcomings, AlON–BN composites were synthesized.[12] Its thermodynamic instability, however, restricts its wide application. Thus, the present authors were motivated to synthesize MgAlON–BN composite ceramics. MgAlON–BN composite ceramics are expected to be structural material candidates used in high temperature and thermal/mechanical shock environments instead of Si_3N_4–BN or Sialon–BN composites. Therefore, it is necessary to investigate the relationship between the physical and

* Corresponding author. Tel.: +46 8 790 8364; fax:+46 8 790 0939.
E-mail address: lidongt@mse.kth.se (L. Teng).

0955-2219/$ – see front matter © 2006 Elsevier Ltd. All rights reserved.
doi:10.1016/j.jeurceramsoc.2006.04.184

mechanical properties of MgAlON–BN compositions and their microstructure.

In the present paper, the physical and mechanical properties of MgAlON–BN composites were investigated at room temperature and at high temperature as functions of h–BN volume fractions, their microstructures were studied using SEM, TEM, HREM and XRD techniques.

2. Experimental procedures

Dense magnesium aluminium oxynitride–boron nitride ($Mg_{0.1}Al_{1.6}O_{2.2}N_{0.2}$–BN) composites with 0–30 vol.% BN were fabricated by hot-pressing technique. The experimental procedures used to manufacture these materials have been described in detail elsewhere[17] and are briefly outlined here. Appropriate amounts of the fine powders of Al_2O_3 (0.5 μm; 99.0% purity; A.R., Beijing Chemical Co., China), AlN (0.5 μm; 98.5% purity with 1.0 wt.% O; Antai High-Technology Ceramics Co., China), MgO (0.5 μm; 99.0% purity; A.R., Beijing Chemical Co., China) and BN (0.1 μm; 98.5% purity with 1.0 wt.% O; Antai High-Technology Ceramics Co., China) were mixed by ball milling in ethanol medium to obtain the homogeneous mixtures. The mixtures obtained this way were placed in a graphite mould and sintered by hot-pressing method at 1800 °C, at 20 MPa for 2 h under N_2 atmosphere. The hot-pressed composites were cut with diamond blade, ground with silicon carbide grounding paper and polished using flannelette with diamond compound abrasive suspension into 3 mm × 4 mm × 40 mm strips perpendicular to the hot-pressing direction. The density of the sample was measured using Archimedes' immersion technique. The three point bending method was introduced to measure room temperature bending strength using a span of 30 mm with a crossing speed of 0.5 mm/min. The standard equations for the strength (σ_f) of a bar in three point bending method are described as follows:[13]

$$\sigma_f = \frac{3}{2} \times \frac{PL}{bw^2} \tag{1}$$

where P is the load force at fracture, L the length of support span, b the specimen width and w is the specimen thickness.

Fracture toughness was measured using the single edge notched beam (SENB) technique, with a notch cut using a 1 mm thick diamond blade producing a notch to depth ratio of 0.25, the loading rate being 0.5 mm/min. The Vickers hardness (H_v) of the composites was calculated from the average results of five indentations performed under a load 98 N on a polished surface of the sample. Fracture toughness and Vickers hardness values were determined using the standard equations[14]

$$K_{IC} = \frac{3}{2} \times \frac{PL}{bw^2} \times Ya^{1/2} \tag{2}$$

and

$$H_v = 1.854 \times \frac{w}{d^2} \tag{3}$$

where a is the notch depth and Y is the dimensionless number, which is dependent on the geometry of the loading and the crack configuration:

$$Y = A_0 + A_1(a/w) + A_2(a/w)^2 + A_3(a/w)^3 + A_4(a/w)^4 \tag{4}$$

with $L/D \approx 8$, $A_0 = +1.96$, $A_1 = -2.75$, $A_2 = +13.66$, $A_3 = -23.98$, $A_4 = +25.22$. Three or five specimens were normally tested to obtain a mean value for above testing experiment.

The crystalline phases of the hot-pressed samples were identified by X-ray diffraction analysis (XRD) (Cu Kα, 1.54060 Å). The measurements were carried out in air with a flow rate of 10 cm^3/min (STP) on a M21X-SRA X-ray diffratometer, manufactured by MAC Science Co. Ltd., Japan, equipped with graphite crystal diffracted-beam monochromator. The accelerating voltage and current were 40 kV and 30 mA, respectively. Intensities were collected by 2θ scanning. PCPDFWIN database was used for indexation of diffractograms. Specimens for transmission electron microscope (TEM) studies were prepared by cutting thin sections perpendicular to hot-pressing direction from the hot-pressed discs. A thin section was then mechanically polished to a thickness of less than 30 μm followed by thinning using a Gatan-600 ion beam thinner at a voltage of 4 kV and perforated. Finally, the ultra-thin plate was sputtered with amorphous carbon to the thickness of about several tens of nanometers. Scanning electron microscope (SEM) specimens were the fracture sections. Gold was sputtered onto the sections and performed on a JSM-6400 microscope equipped with energy dispersive spectroscopy detector (EDS; INCA, Oxford Instrument). The accelerating voltage determining the energy and wavelength of electrons in the electron beam is 35 kV. The resolution in the secondary electron mode at 35 kV will be 3.5 nm at a working distance of 8 mm. Machinability was evaluated using hard metal alloy drill bits under the varied conditions.

3. Experimental results

3.1. Phase analysis of MgAlON/h–BN composites

Fig. 1 illustrates XRD patterns of pure MgAlON and MgAlON-30 vol.% h–BN composites synthesized by hot-pressing technique at 1800 °C in N_2 atmosphere for 2 h under the pressure of 20 MPa. The XRD spectra identified that the main phase was MgAlON, the second was h–BN phase and no impurities have been detected with regards to the detection limit of XRD technique. A further examination of the same sample by TEM, as can be seen from Fig. 2 that shows h–BN has rod-like or flake structure due to growth of h–BN along (0 0 2) direction and is dispersed within MgAlON grain boundaries. MgAlON and h–BN were indexed as a cubic and hexagonal cells.

3.2. Mechanical properties of MgAlON/h–BN composites

The effect of h–BN addition on Vickers hardness, density, room temperature bending strength and fracture toughness of MgAlON/h–BN composites were investigated. Fig. 3 shows

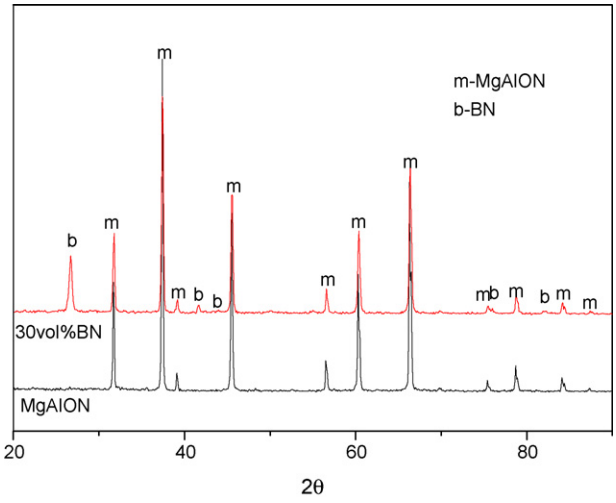

Fig. 1. XRD patterns taken on the crushed powders of pure MgAlON and MgAlON–15 vol.% h–BN composites.

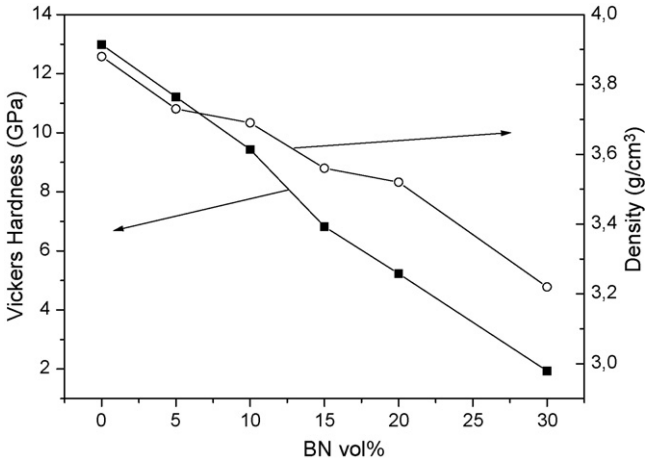

Fig. 3. Vickers hardness and density as a function of BN content.

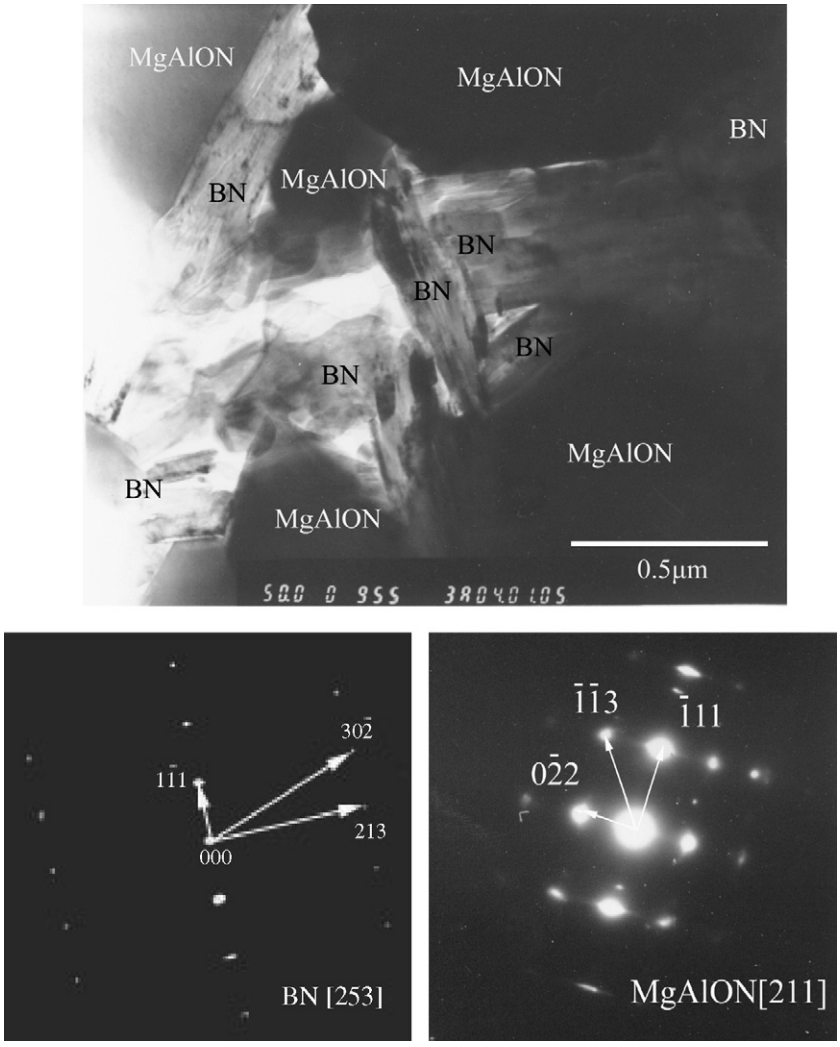

Fig. 2. TEM photographs and diffraction pattern of MgAlON–BN with an addition of 15 vol.% h–BN.

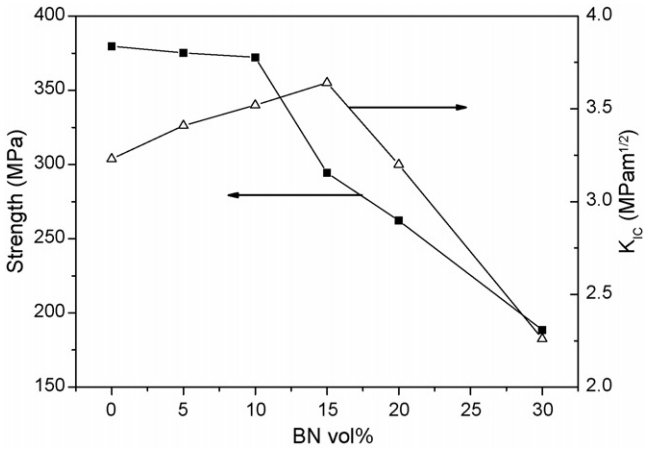

Fig. 4. Strength and fracture toughness as a function of BN content.

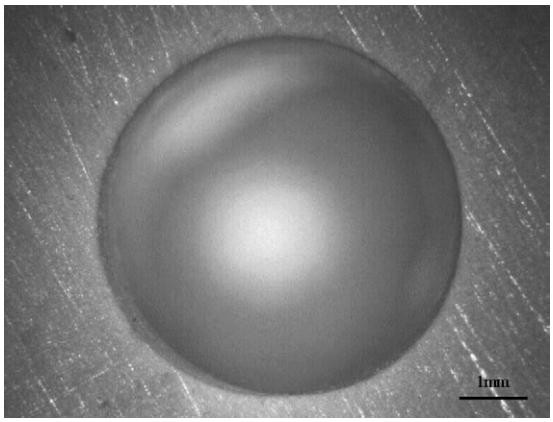

Fig. 7. Macrograph of a typical drill hole in the MgAlON/15 vol.% h–BN.

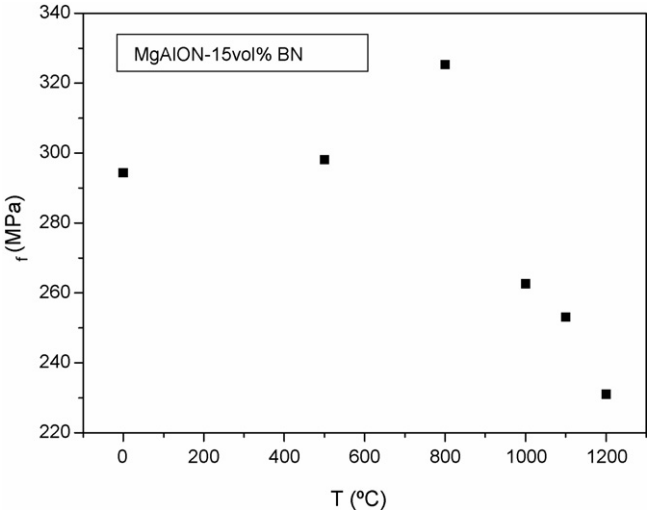

Fig. 5. Temperature dependence of bending strength of MgAlON/15 vol.% BN sample in argon.

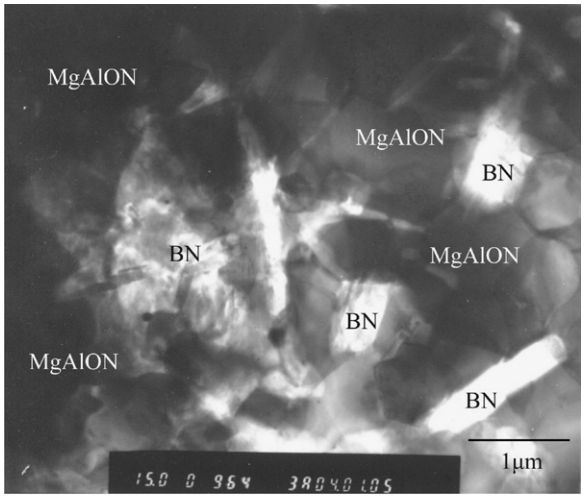

15vol% h-BN

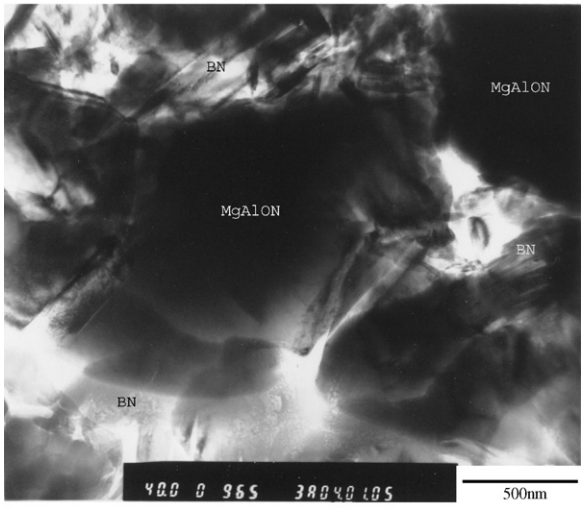

30vol% h-BN

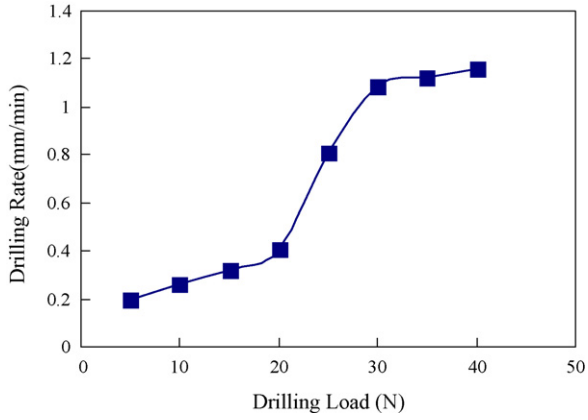

Fig. 6. Measurements of drilling rate as a function of normal force for MgAlON/15 vol.% h–BN composite ceramics.

Fig. 8. TEM micrographs with different h–BN contents of (a) 15 and (b) 30 vol.%, respectively.

Vickers hardness and density of the composite ceramics sintered at 1800 °C for 2 h as a function of h–BN volume content. The Vickers hardness and density of MgAlON/h–BN composite ceramics decreased with an increase of h–BN volume fraction. The Vickers hardness of MgAlON/h–BN with 15% h–BN volume fraction is as high as $H_v = 6.82$ GPa, which matches the requirements for machining.[15,16]

Fig. 4 shows room temperature bending strength and fracture toughness of samples sintered at 1800 °C for 2 h as a function of h–BN volume fraction. The room temperature bending strength of MgAlON/h–BN composite ceramics decreased with an increase of h–BN volume fraction, this may be explained by the fact that h–BN particles might prevent the formation of MgAlON as well as the contact between MgAlON grains and accordingly restrain the sintering of the composite due to the non-reactive nature of BN. However, the fracture toughness of MgAlON/h–BN composite ceramics increased with increasing of h–BN content, reaching a maximum of 3.64 MPa $m^{0.5}$ and then decreased considerably.

3.3. Temperature dependence of bending strength

Fig. 5 shows the temperature dependence of bending strength of MgAlON/15 vol.% h–BN in argon gas. As can be seen, bending strength increased with increasing temperature and reached a maximum of 325.3 MPa at 800 °C, then decreased to 231.04 MPa at 1200 °C. The reason for the improved bending strength will be linked to the large difference in thermal

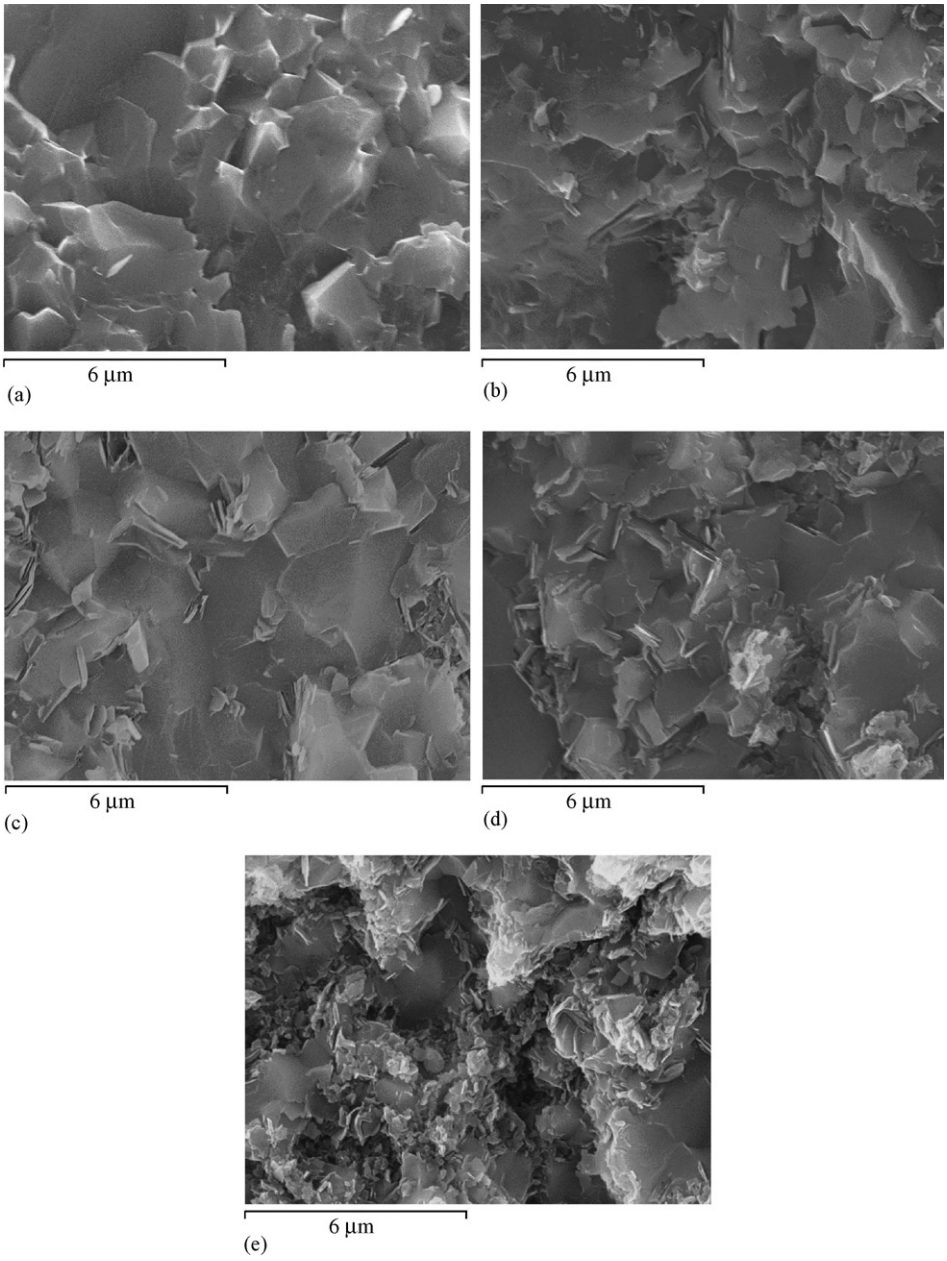

Fig. 9. Fracture section morphology by SEM hot-pressed at 1800 °C for 2 h. (a) 0, (b) 5, (c) 10, (d) 15 and (e) 30%.

expansion coefficient between MgAlON and BN and discussed in Section 4.2.

3.4. Machinability

The MgAlON/h–BN composite ceramics containing more than 15 vol.% h–BN exhibited excellent machinability, which is very important for practical applications of engineering ceramics, as can be seen from Fig. 6. Machinability improved with increasing h–BN volume fractions.

One photograph of a series of typical drill holes in the MgAlON/h–BN composite containing 15% volume fraction h–BN is shown in Fig. 7. No crack was found around the edge of the drilled holes. Load force on the drill bit varied in the range of 5–40 N at a fixed drill revolution rate of 400 rpm. Drilling depths were approximately 4 mm. Each test was measured three times under the same conditions. A new drill bit was used at the beginning of each set to avoid systematic effects due to wearing of the drill. Drilling rates show a non-linear relation with the load in the experimental range, as shown in Fig. 6. When the load on the drill bit reached to 30 N, a satisfactory drill rate can be obtained. The surface toughness of the drilled section was $3.0 \pm 0.2\ \mu m$, measured by a microscope under the conditions that satisfied a fixed load of 10 N on the drill bit. No significant cracks were observed on the surface.

4. Discussion

4.1. Microstructure evolution of MgAlON/BN composites

The TEM results shown in Fig. 8 indicated that the MgAlON phase was continuous in a composite when BN amount was 15 vol.%. However, addition of 30 vol.% BN leads to discontinuous microstructural network. In the process of synthesizing MgAlON–BN composites, it was considered that pressure was transmitted through Al_2O_3, AlN and MgO powders when the BN content was lower than 20 vol.%. This resulted in a continuous microstructure with MgAlON. The pressure, however was partially transmitted through BN powders when BN is more than 30 vol.%, which would lead to the discontinuous microstructure.[17] Fig. 9 shows scanning electron micrographs of fracture surfaces of sintered MgAlON/h–BN composites without BN as well as with 5, 10, 15, 20 and 30 vol.% h–BN additions. These surfaces represent planes perpendicular to the hot-pressing direction. The fracture modes for MgAlON and composites containing 5 vol.% BN were found to be a mixed transcrystalline and intercrystalline; for composites containing 15 and 30 vol.% BN, however, the mode was found to be a mixed intercrystalline and cleavage fracture. Equiaxed MgAlON grains, about 2–3 μm in size, were observed in monolithic MgAlON and MgAlON/h–BN composites containing different h–BN volume fraction. Hexagonal–BN, about 200–300 nm in thickness as well as 1–3 μm in length, grew in flake shape configuration and it was evident that BN grains were preferentially oriented with the basal plane perpendicular to the direction of hot-pressing, as can be seen from Fig. 8. Experimental observations revealed that the hexagonal BN flakes were homogeneously dispersed among MgAlON grain boundaries. HREM results indicate that MgAlON grains bonded directly. Some glass phase however, is located at the grain boundary or junction nodes between MgAlON and BN grains, as can be seen from Fig. 10. EDS analysis of the glass shows that it is rich in boron and oxygen. This suggests that BN absorbed some oxygen to yield B_2O_3 during the synthesis process.

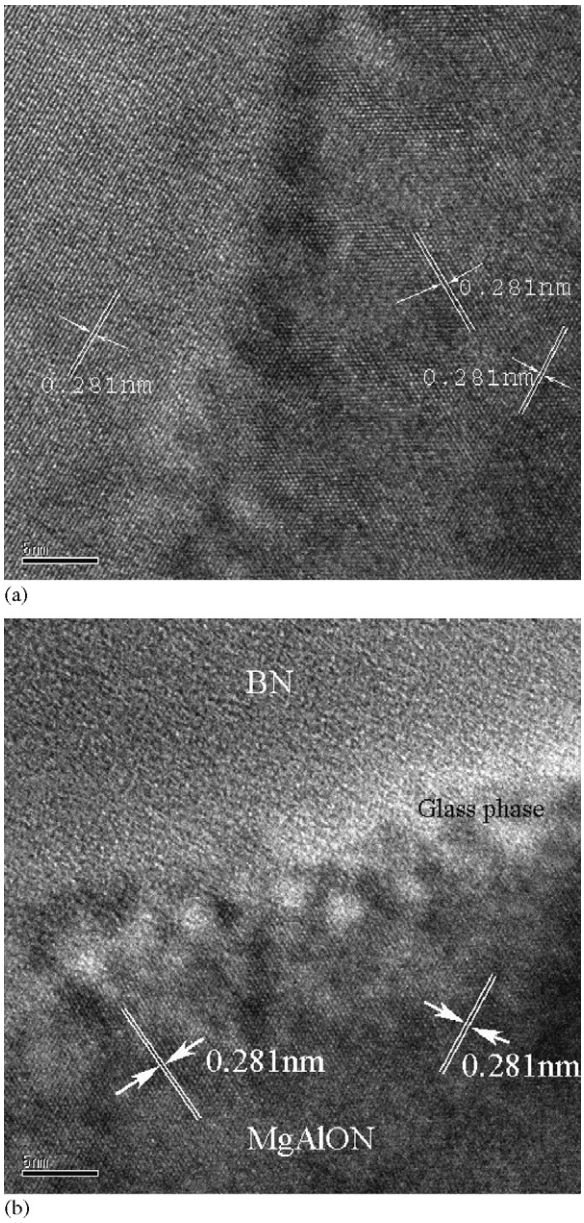

Fig. 10. HREM images of the interfaces between (a) MgAlON and (b) MgAlON/BN.

4.2. The effect of BN addition on mechanical properties

As is known, h–BN has low density, hardness, low Young's modulus in addition to the non-active nature. The presence of an inert BN phase in the MgAlON matrix which has limited sinterability decreases the densification rate of the composites. These resulted in the decrease of density, hardness, Young's modulus

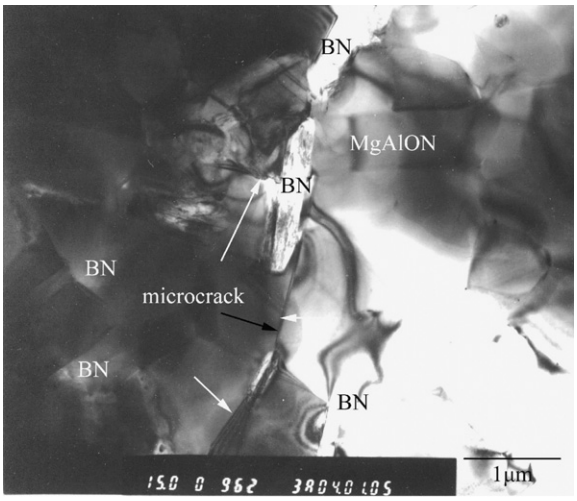

(a) crack deflection

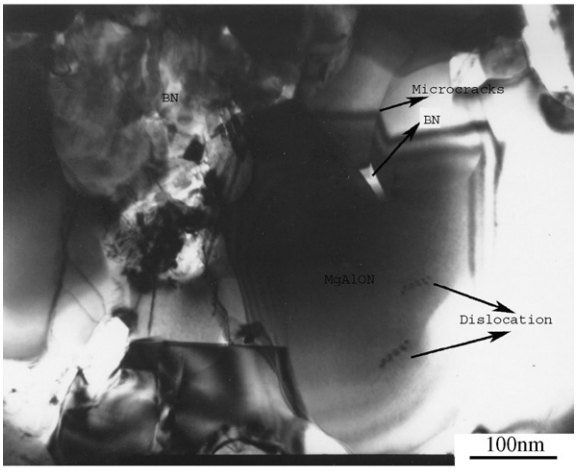

(b) grain boundary

Fig. 11. TEM micrographs of (a) crack deflection and (b) grain boundary dislocation in sample with 15 vol.% h–BN.

of composite ceramics with increasing BN volume fraction and consequently led to the decrease of bending strength. Another pronounced microstructural feature in the present MgAlON–BN composites is the presence of high densities of microcracks near the interface between MgAlON and BN and the dislocations, as can be Fig. 11. The morphological characteristic of the microcracks revealed that these caused by the thermal expansion coefficient mismatch between MgAlON and BN or the anisotropic character of h–BN. Thermal expansion coefficient of BN in one direction ($\alpha_{//} = 7.51 \times 10^{-6}\,K^{-1}$) is larger than most oxides; the other direction is very small($\alpha_{\perp} = 1 \times 10^{-6}\,K^{-1}$). The thermal expansion coefficient of MgAlON is $5.31 \times 10^{-6}\,K^{-1}$. These microcracks would have pronounced negative effect on the bending strength at room temperature. However, in the process of fracture of composites, as a propagating crack reaches a BN flake, the stresses acting on the crack-tip will change from three dimensions to two dimensions because of the h–BN flakes. Hence, the crack-tip is blunted and deflected and the deflection will consume much energy in this process, which is positive for the fracture toughness, but negative for room bending strength. In addition, the pullout effect is contributing to the increase of work of fracture toughness. But the BN addition beyond 20 vol.% produced the microstructure change and the defects would also increase due to the non-reactive nature of BN. Thus, the microcracks were limited to increase the fracture toughness in this case and consequently the fracture toughness decreased corresponding. However, the composite ceramics expand considerably at elevated temperature and consequently the residual stress and microcracks decreased in consequence. On the other hand, h–BN interwoven microstructure of composites containing 15 vol.% BN prevented grain boundary slip and reduced the attenuation rate of high temperature strength. These result in increasing of the bending strength, reaching the maximum value at 800 °C. The softening of non-crystalline at high temperature leads to the decrease of bending strength. Furthermore, the new microcracks may be formed due to the continuous expansion with increasing temperature and consequently leads to the decrease of bending strength. The convenience of machining is presumably attributed to the cleavage of the layered structure h–BN dispersed in the matrix, which may confine the machining damage to a very small region under the tip of the tools through microcracking to absorb and disperse the force during the machining operations. Linking of the microcracks results in the ease of machining.

It should be pointed out that BN particles would like to stick together easily to form agglomerates. One possible reason for the agglomeration of BN particles is that only a small amount of liquid is produced due to the oxidation of BN at very low oxygen partial pressure during the sintering process. Thus, inhomogeneity of the formation and distribution of the liquid phase resulted in the presence of local regions of liquid in the microstructure and poor wetting in the neighboring regions. Therefore,

Fig. 12. Groups of nano-sized grains of BN agglomerates.

the local liquid pools give high density regions surrounded by poorly sintered regions and porosity and nano-sized grains. This microstructure must influence the mechanical properties of the material and porosity and consequently is detrimental to the strength and fracture toughness of the composite and may act as fracture flaw, as can be seen from Fig. 12. These phenomena have also been observed in TiN based composite ceramics.[18]

From microstructural analysis, it can be seen that bending strength at room temperature and elevated temperature as well as fracture toughness of MgAlON/h–BN are closely related to its microstructure. Thus, in order to obtain a high performance MgAlON/h–BN composite materials, some improvements are needed. First, a homogeneous microstructure is asked, which can be realized by controlling the morphological and chemical characterization of starting powders. Secondly, a proper BN addition would be suitable in order to control the microstructure and the thermal mismatch between MgAlON matrix and h–BN flakes when the composite material is cooled to room temperature.

5. Conclusion

(1) MgAlON/h–BN structural material was fabricated by hot-pressing technique. The SEM and TEM observations revealed that h–BN were homogeneously dispersed within the MgAlON grain boundary. HREM results indicate that MgAlON grains bounded directly. Some glass phase however, is located at the grain boundary or junction nodes between MgAlON and BN grains.
(2) There was a significant decrease in the bending strength, Vickers hardness and density with increasing h–BN content due to the low density and poor densification behavior of h–BN. The enhancement of the fracture toughness was mainly attributed to the interwoven microstructure of h–BN and the microcracks induced by expansion coefficient mismatch between MgAlON and h–BN.
(3) The bending strength was found to increase with increasing temperature and reaching the maximum value at 800 °C, then decrease to 231 MPa at 1200 °C.
(4) The observed excellent machinability of MgAlON–BN containing 15 vol.% BN derived from the cleavage effect of the h–BN crystals as well as the weak interfacial bond between MgAlON matrix and the h–BN.

Acknowledgements

The present authors express their gratitude to Prof. S. Seetharaman for his valuable comments and discussions and also thank National Nature Science Foundation of China of Nos. 50332010 and 50425415 for financial support on the sample preparation and mechanical property testing.

References

1. Zhang, G. J. and Jin, Z. Z., Toughening mechanisms of particulate composite ceramics. *J. Chin. Ceram. Soc.*, 1994, **22**(3), 259–268 [in Chinese].
2. Guan, Z. D. and Zhang, Z. T., *Physical Properties of Inorganic Materials*. Tsinghua University, 1998 [in Chinese].
3. Gong, J. H., Guan, Z. D. and Wu, J. J., R-curve behavior of indentation cracks in silicon nitride based ceramics composites. *J. Non-Cryst. Solids*, 1994, **177**, 46–53.
4. Zhang, G. J. and Jin, Z. Z., Toughening mechanisms of particulate composite ceramics. *J. Chin. Ceram. Soc.*, 1994, **22**(3), 259–268 [in Chinese].
5. Padture, N. P., Christopher, J. E., Hockin, H. K. Xu and Lawn, B. R., Enhanced machinability of silicon carbide via microstructure design. *J. Am. Ceram. Soc.*, 1995, **78**(1), 215–217.
6. Wang, R. G., Pan, W. and Jiang, M. N., Investigation of the physical and mechanical properties of hot-pressed machinable Si_3N_4/h-BN composites and FGM. *Mater. Sci. Eng. B*, 2002, **90**, 261–268.
7. Coblenz, W. S. and Lewis III, D., In situ synthesis of B_2O_3 with AlN and /or Si_3N_4 to form BN-toughened composites. *J. Am. Ceram. Soc.*, 1988, **71**(12), 1080–1085.
8. Mazdiyasni, K. S. and Ruh, R., High/low modulus Si_3N_4-BN composite for improved electrical and thermal shock behavior. *J. Am. Ceram. Soc.*, 1981, **64**(7), 415–419.
9. Lutz, E. H. and Swain, M. V., Fracture toughness and thermal shock behavior of silicon nitride-boron nitride ceramics. *J. Am. Ceram. Soc.*, 1992, **75**(1), 67–70.
10. Hayama, S., Ozawa, M. and Suzuki, S., Thermal shock fracture behavior and fracture energy of Sialon-BN composites. *J. Ceram. Soc. Jpn.*, 1996, **104**, 828–831.
11. Maeda, E., Aratani, K., Kawasaki, T. and Kishidaka, H., Erosion of Si_3N_4-Al_2O_3 sintered articles by molten steel. *J. Ceram. Soc. Jpn.*, 1980, **88**, 523–531.
12. Shimpo, A., Ide, H. and Ueki, M., ALON and its composite ceramics. *J. Ceram. Soc. Jpn.*, 1992, **100**, 504–508.
13. Standard test method for flexural strength of advanced ceramics at ambient temperature. In *Annual Book of ASTM Standards*, Designation: C1161-90, vol. 15.01, ASTM, West Conshohock, PA, 1990, pp. 327–333.
14. Niihara, K., Morena, R. and Hasselman, D. P. H., Evaluation of K_{IC} of brittle solids by the indentation method with low crack-to-indent ratios. *J. Mater. Sci. Lett.*, 1982, **1**, 13–16.
15. Hockin, H. K. Xu and Jahanmir, S., Scratching and grinding of a machinable glass-ceramic with weak interfaces and rising T-curve. *J. Am. Ceram. Soc.*, 1995, **78**(2), 497–500.
16. El-Raghy, T., Chakraborty, S. and Barsoum, M. W., Synthesis and characterization of Hf_2PbC, Zr_2PbC and M_2SnC(M = Ti, Hf Nb or Zr). *J. Eur. Ceram. Soc.*, 2000, **20**, 2619.
17. Zhang, Z.T., Wang, X.D., Li, W.C. and Seetharaman, S., Synthesis and characterization of MgAlON-BN composites, Z. Metallkde (2006), in press.
18. Xu, F. F., Wen, S. L., Norsberg, L. O. and Ekstrom, T., TEM study of Y-doped α-Sialon composites with 10 vol% TiN particulates. *Mater. Lett.*, 1998, **34**, 248–252.